

Water–Protein Interactions of an Arginine-Rich Membrane Peptide in Lipid Bilayers Investigated by Solid-State Nuclear Magnetic Resonance Spectroscopy

Shenhui Li, Yongchao Su, Wenbin Luo, and Mei Hong*

Department of Chemistry, Iowa State University, Ames, Iowa 50011

Received: December 31, 2009; Revised Manuscript Received: February 16, 2010

The interaction of an arginine (Arg) residue with water in a transmembrane antimicrobial peptide, PG-1, is investigated by two-dimensional heteronuclear correlation (HETCOR), solid-state nuclear magnetic resonance (NMR) spectroscopy. Using ^{13}C and ^{15}N dipolar-edited ^1H – ^{15}N HETCOR experiments, we unambiguously assigned a water–guanidinium cross-peak that is distinct from intramolecular protein–protein cross-peaks. This water–Arg cross-peak was detected within a short ^1H spin diffusion mixing time of 1 ms, indicating that water is in close contact with the membrane-inserted guanidinium. Together with previously observed short guanidinium–phosphate distances, these solid-state NMR data suggest that the Arg side chains of PG-1 are stabilized by both hydration water and neutralizing lipid headgroups. The membrane deformation that occurs when water and lipid headgroups are pulled into the hydrophobic region of the bilayer is symptomatic of the membrane-disruptive function of this antimicrobial peptide. The water–Arg interactions observed here provide direct experimental evidence for molecular dynamics simulations of the solvation of Arg side chains of membrane proteins by deeply embedded water in lipid bilayers.

Introduction

Water–protein interactions are ubiquitous in biological systems and play an important role in the folding, stability, and function of proteins. Nuclear magnetic resonance (NMR) has long been used to investigate protein–water interactions and the mechanisms of polarization transfer from water to proteins.¹ For microcrystalline proteins in the solid-state, magic-angle-spinning (MAS) NMR experiments have shown that water–protein magnetization transfer can be mediated by chemical exchange followed by dipolar spin diffusion,² nuclear Overhauser effects (NOE) between water and the protein,^{3,4} and rotating-frame Overhauser effects.⁵ For proteins bound to phospholipid bilayers, the balance between the interaction of polar residues with water and the interaction of hydrophobic residues with lipid acyl chains fundamentally determines the membrane topology of the protein. For membrane proteins that conduct ions across lipid bilayers, protein interactions with both membrane-surface water and channel water are important for the oligomeric structure and the function of the ion channel.

Several spin diffusion solid-state NMR (SSNMR) experiments have been introduced to determine the distances of proteins to membrane-associated water and to lipid chains.^{6–8} The focus of these experiments has been to determine the global topology and conformational feature of the membrane proteins: whether they are transmembrane (TM) or surface-bound⁷ and how the water accessibility of the protein changes with environmental conditions.⁹ Thus, most of these experiments employed relatively long spin diffusion mixing times of tens to hundreds of milliseconds, which detect water or lipid chain magnetization that originated from as far as several nanometers away. At these long mixing times, these experiments do not give site-specific information about water molecules within hydrogen bonding distance to protein residues.

Amino acids with ionizable side chains such as arginine (Arg) play important roles in the function of many membrane peptides and proteins, such as voltage-gated potassium channels,^{10–12} antimicrobial peptides,^{13,14} and cell-penetrating peptides.¹⁵ There has been great interest in understanding how the positively charged Arg side chains are inserted into the hydrophobic part of the lipid membrane against high-free-energy barriers.¹⁶ A number of molecular dynamics (MD) simulations have been carried out to address this question.^{17–22} Freitas et al. found that a stabilizing hydrogen-bonded network of water and lipid phosphates around the arginines of the S4 helix of a voltage-gated potassium channel reduced the local thickness of the bilayer hydrocarbon core to about 10 Å.¹⁷ Herce et al. showed that water penetrated the lipid bilayer and solvated the charged arginine and lysine residues during the translocation of the HIV Tat peptide across the membrane.²⁰ Allen et al. found that the Arg side chain in a poly-Leu helix remained protonated in the membrane as a result of the stabilizing effects of membrane deformations.²³ Compared to MD simulations, direct experimental evidence for Arg interaction with water remains scarce^{13,24,25} due to the general difficulty of obtaining high-resolution structure information of membrane proteins in the disordered environment of lipid bilayers.

PG-1 is an Arg-rich, disulfide-linked, β -hairpin, antimicrobial peptide found in porcine leukocytes.^{26,27} Extensive biochemical assays^{28–30} and neutron diffraction data³¹ have shown that PG-1 carries out its antimicrobial function by forming pores in the microbial cell membrane, thus disrupting the membrane barrier function. Solid-state NMR ^1H and ^{19}F spin diffusion data revealed that PG-1 self-assembles into a TM oligomeric β -barrel in bacteria-mimetic POPE/POPG membranes.³² ^{13}C – ^{31}P distance constraints indicate that the Arg residues in these β -barrels are complexed with lipid phosphates, and the guanidinium is within hydrogen bonding distance to the lipid ^{31}P .^{13,25} These results indicated that charge neutralization by lipid phosphates is a mechanism with which the Arg-rich PG-1 reduces the free energy of insertion into the hydrophobic region of the mem-

* Corresponding author. Phone: 515-294-3521. Fax: 515-294-0105. E-mail: mhong@iastate.edu.

brane. However, no experimental data has yet been reported about whether PG-1 uses water to stabilize its structure in the membrane, as suggested by MD simulations of other Arg-rich membrane peptides.

In this work, we investigate the water–Arg interaction of PG-1 in POPE/POPG bilayers using heteronuclear correlation (HETCOR) NMR. We describe how a spectral editing technique that removes protein ^1H signals allows the unambiguous identification of the resonances of water protons in contact with the Arg side chains. This dipolar editing is essential for nondeuterated proteins, whose backbone $\text{H}\alpha$ and amino protons often resonate within the possible water ^1H chemical shift range. We show how the use of short spin-diffusion mixing times combined with dipolar editing allows us to detect water that is specifically associated with a guanidinium in the membrane.

Materials and Methods

Sample Preparation. $\text{U-}^{13}\text{C}$, ^{15}N -labeled Arg•HCl was purchased from Sigma Aldrich (St. Louis, MO). A PG-1 sample ($\text{NH}_2\text{--RGGRLCYCRRRFCVCVGR--CONH}_2$) containing $\text{U-}^{13}\text{C}$, ^{15}N -labeled Arg₄ and ^{15}N -labeled Leu₅ (R4, L5–PG-1) was synthesized and reconstituted into POPE/POPG membranes as described before.²⁵ Briefly, 1-palmitoyl-2-oleoyl-*sn*-glycero-3-phosphatidylethanolamine (POPE) and 1-palmitoyl-2-oleoyl-*sn*-glycero-3-phosphatidylglycerol (POPG) were mixed at a 3:1 molar ratio in organic solvents and lyophilized. The lipid powder was suspended in water and subjected to five cycles of freeze–thawing to form lipid vesicles. The peptide solution was mixed with the lipid vesicle solution at a peptide–lipid molar ratio of 1:12.5. The mixture was incubated at 303 K overnight, then centrifuged at 55 000 rpm to obtain a ~40% hydrated pellet, which was packed into a 4 mm MAS rotor for SSNMR experiments.

Solid-State NMR Spectroscopy. SSNMR experiments were carried out on a Bruker AVANCE-600 (14.1 T) spectrometer using a 4 mm triple-resonance MAS probe. Temperatures were controlled using a Bruker BCU-Xtreme unit. Radio frequency pulse lengths were typically 5–6 μs for ^{13}C , 6 μs for ^{15}N , and 3.0–4.5 μs for ^1H .

For the model compound $\text{U-}^{13}\text{C}$, ^{15}N -Arg•HCl, all ^1H – ^{15}N and ^1H – ^{13}C Lee–Goldburg (LG) HETCOR experiments (Figure 1a) were carried out at 273 K under 7.5 kHz MAS. ^1H homonuclear decoupling was achieved using the FSLG sequence³³ with an 80 kHz transverse field. The ^1H chemical shift scaling factor due to the FSLG sequence was directly measured on the model peptide N-formyl- $\text{U-}^{13}\text{C}$, ^{15}N -labeled Met-Leu-Phe–OH (MLF)³⁴ to be 0.560. For ^1H – ^{15}N LG-HETCOR experiments, a LG cross-polarization (CP) contact time of 800 μs and a maximum ^1H evolution time of 5.1 ms were used. For ^1H – ^{13}C LG-HETCOR experiments, the LG-CP contact time was 300 μs , and the maximum t_1 evolution time was 4.1 ms. The MELODI–HETCOR experiment with two rotor periods of dipolar dephasing (Figure 1c) was carried out at 273 K under 6859 Hz MAS. The ^{13}C and ^{15}N 180° pulse lengths were 12 μs . Hartman–Hahn (HH) CP with a contact time of 800 μs was used to allow ^1H spin diffusion. To further promote ^1H spin diffusion, an additional z -filter period of 1 ms was used. Since the ^1H – ^1H dipolar coupling during HH-CP is half the strength of laboratory-frame dipolar coupling, the total effective spin diffusion time of this experiment for Arg•HCl was 1.4 ms.

For the membrane-bound R4, L5–PG-1 sample, ^1H – ^{13}C and ^1H – ^{15}N LG-HETCOR experiments were carried out under 7.5 kHz MAS at 283 K. The LG-CP contact time was 800 μs . For the spin-diffusion-active ^1H – ^{15}N HETCOR experiment (Figure

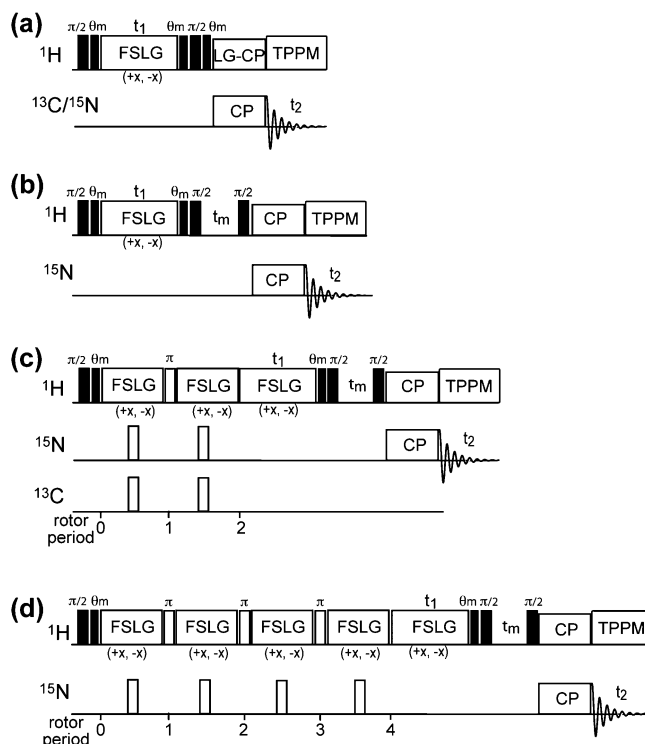


Figure 1. Pulse sequences for various HETCOR and MELODI–HETCOR experiments. (a) 2D LG-CP HETCOR. (b) 2D HH-HETCOR with ^1H spin diffusion. (c) 2D MELODI–HETCOR with two rotor periods of ^{13}C and ^{15}N dipolar dephasing. (d) 2D MELODI–HETCOR with four rotor periods of ^{15}N dephasing.

1b), we used HH-CP with no additional ^1H mixing period. The HH-CP contact time was 2 ms at 283 K, corresponding to an effective spin diffusion time of 1 ms. The ^{15}N -detected and ^{13}C , ^{15}N -dephased MELODI–HETCOR experiment was carried out under 6859 Hz MAS with 2 ms HH-CP without further spin diffusion mixing. Most MELODI–HETCOR experiments used two rotor periods for dipolar dephasing. To better suppress the mobile side chain proton signals, we also carried out a MELODI–HETCOR experiment with four rotor periods of ^{15}N dipolar dephasing (Figure 1d). Additional HETCOR experiments at 253 K largely confirmed the 283 K data and thus are not shown here.

^{13}C chemical shifts were referenced to the α -Gly C' signal at 176.49 ppm on the TMS scale, and ^{15}N chemical shifts were referenced to the ^{15}N signal of N-acetylvaline at 122.0 ppm on the liquid ammonia scale. The ^1H chemical shifts were externally referenced to those of MLF.³⁵

Results

2D Heteronuclear Correlation Experiments for Detecting Water–protein Interactions. The ^1H chemical shift of water can vary between 0 and 10 ppm, depending on the extent of hydrogen bonding among water molecules and between water and other polar functional groups.^{36,37} Thus, to correctly identify the water–protein correlation, it is necessary to distinguish the water and protein ^1H resonances. The protein ^1H chemical shifts can be readily assigned using 2D ^1H – ^{15}N and ^1H – ^{13}C HETCOR experiments with spin-diffusion-free LG-CP³⁸ for polarization transfer (Figure 1a). Combined with homonuclear-decoupled ^1H chemical shift evolution, these pulse sequence elements ensure that mostly only one-bond correlation peaks are observed in the 2D spectra. To obtain correlations between nondirectly bonded protons and ^{13}C or ^{15}N , we use a short ^1H spin-diffusion

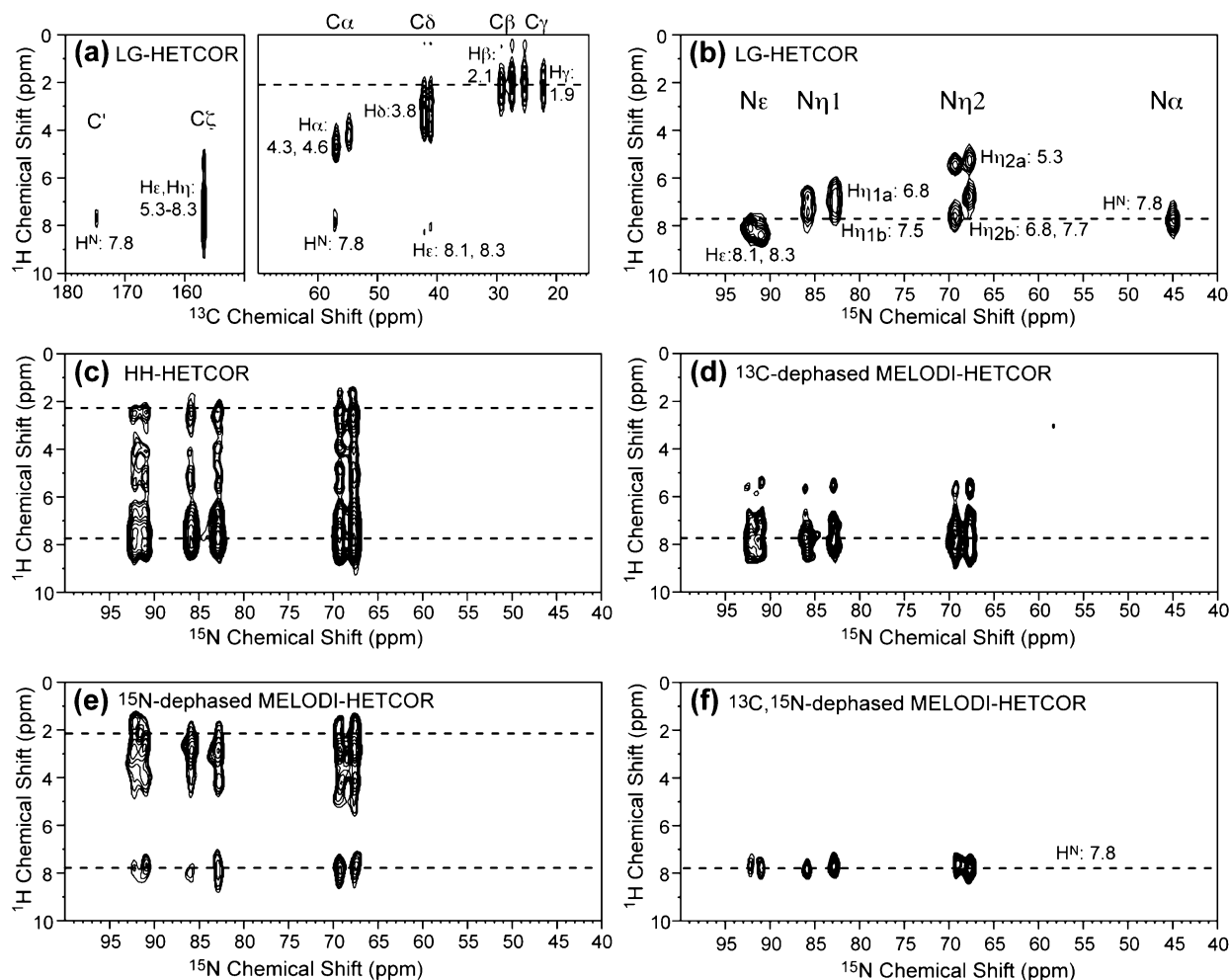


Figure 2. 2D HETCOR and MELODI–HETCOR spectra of U-¹³C, ¹⁵N-labeled Arg·HCl. (a) ¹H–¹³C LG-CP HETCOR. (b) ¹H–¹⁵N LG-CP HETCOR. (c) ¹H–¹⁵N HH-HETCOR with 1.4 ms spin diffusion. (d) ¹H–¹⁵N MELODI–HETCOR with two rotor periods of ¹³C dephasing. (e) ¹H–¹⁵N MELODI–HETCOR with two rotor periods of ¹⁵N dipolar dephasing. (f) ¹H–¹⁵N MELODI–HETCOR with two rotor periods of simultaneous ¹³C and ¹⁵N dephasing.

mixing period, HH-CP for polarization transfer (Figure 1b), or both, during which ¹H spin diffusion proceeds at half the rate of the laboratory-frame spin diffusion. Thus, the HH-HETCOR experiment can exhibit cross-peaks of ¹³C/¹⁵N spins with peptide protons several bonds away as well as with neighboring water protons.

We distinguish protein and water protons using a ¹³C/¹⁵N dipolar dephasing period before ¹H evolution (Figure 1c). This technique, termed medium- and long-distance (MELODI) HETCOR,^{39,40} was introduced previously for spectral editing of protein HETCOR spectra. During the dipolar dephasing period, ¹H magnetization evolves under ¹³C–¹H or ¹⁵N–¹H dipolar couplings or both, which are recoupled by alternating 180° pulses on the ¹H and heteronuclear channels in the same fashion as rotational echo double resonance (REDOR) experiments.⁴¹ ¹H homonuclear decoupling and a central ¹H 180° pulse maintain the ¹H magnetization and suppress any ¹H chemical shift evolution. The MELODI dephasing pulses can be applied on one or both heteronuclear spins. Simultaneous ¹³C and ¹⁵N irradiation ensures that the signals of both aliphatic and amino protons of U-¹³C, ¹⁵N-labeled protein residues are suppressed while the signals of water protons survive.

For mobile functional groups with attenuated C–H and N–H dipolar couplings, the two rotor periods of MELODI dephasing may not be sufficient to suppress their signals. In that case, one

can readily extend the MELODI dephasing time to four rotor periods or longer to augment the dipolar dephasing effect (Figure 1d).

HETCOR Experiments of U-¹³C, ¹⁵N Labeled Arg·HCl. Figure 2a,b shows 2D ¹H–¹³C and ¹H–¹⁵N LG-HETCOR spectra of U-¹³C, ¹⁵N-labeled Arg·HCl. This crystalline compound has two inequivalent molecules in the asymmetric unit cell;⁴² thus, two sets of ¹³C and ¹⁵N chemical shifts were observed in the spectra. These ¹³C and ¹⁵N LG-HETCOR spectra allowed the assignment of all ¹³C, ¹⁵N, and ¹H chemical shifts (Table 1).⁴³

All protons in U-¹³C, ¹⁵N-labeled Arg·HCl are directly bonded to a ¹³C or a ¹⁵N spin; thus, ¹³C and ¹⁵N dipolar dephasing should suppress the one-bond peaks of all rigid segments and leave only the signals of mobile segments. The effective dipolar couplings in a two-rotor-period MELODI experiment are $\delta_{\text{XH}}^{\text{eff}} = \delta_{\text{XH}}^{\text{rigid}} \times 4 \times 0.577 \times S_{\text{XH}}$ where 0.577 is the theoretical FSLG scaling factor, and the rigid-limit couplings were 22.7 kHz for C–H and 10.6 kHz for N–H bonds. The order parameters S_{XH} account for any segmental motion that may be present and have been previously measured for Arg·HCl to be 0.91, 1.02, 0.96, 1.03, and 0.43 for Cα–Hα, Cδ–Hδ₂, Nε–Hε, Nη–Hη₂, and Nα–H^N, respectively,⁴⁴ which give effective dipolar couplings of 47.7, 53.2, 23.5, 25.2, and 10.5 kHz. Since ¹H magnetization evolves during the MELODI

TABLE 1: ^1H , ^{13}C , and ^{15}N Isotropic Chemical Shifts (ppm) of Crystalline Arg \cdot HCl at 273 K and Arg $_4$ of PG-1 Bound to POPE/POPG Membranes at 283 K

site	Arg \cdot HCl	Arg $_4$ in PG-1
N α	44.8	117.6
N ϵ	92.2, 90.9	84.1
N η 1	85.7, 82.6	72.4
N η 2	69.3, 67.7	
C'	175.9, 174.7	171.3
C α	56.8, 54.7	51.5
C β	29.1, 27.3	
C γ	25.2, 22.1	
C δ	42.0, 41.0	40.5
C ζ	156.7	156.6
H N	7.8	7.9
H α	4.6, 4.3	4.7
H β	2.1	1.8
H γ	1.9	1.3
H δ	3.8	2.9
H ϵ	8.1, 8.3	6.4
H η 1	6.8, 7.5	6.3
H η 2	5.3, 6.8, 7.7	
H $_2\text{O}$		4.8

dephasing period, the spin dynamics is that of two-spin $I-S$ systems, even for CH_2 , NH_2 , and NH_3 groups. Figure 3a shows the calculated C–H and N–H MELODI dephasing curves as a function of the position of the ^{13}C or ^{15}N 180° pulses.³⁹ When the dephasing pulses are at the center of the rotor period, the H α , H δ , H ϵ , and H η intensities are all near zero (-6% to 1% of the full intensities) and, thus, are negligible in the MELODI–HETCOR spectrum. The only exception is the amino protons H N , whose three-site jump motions attenuate the ^1H – ^{15}N dipolar couplings so that $\sim 50\%$ of the intensities remain with the 180° pulses at the center of the rotor period.

Figure 2c shows the ^1H – ^{15}N HETCOR control spectrum in the absence of ^{13}C and ^{15}N dephasing pulses. All one-bond cross-peaks and multiple-bond cross-peaks, such as ^{15}N to aliphatic correlations, are observed. When ^{13}C dephasing pulses are turned on, the aliphatic ^1H signals between 1.0 and 5.0 ppm are completely suppressed, while the amino ^1H signals between 5.0 and 9.0 ppm remain (Figure 2d). When the ^{15}N dephasing pulses are turned on, the H ϵ and H η peaks between 5 and 7 ppm decreased in intensity, while the aliphatic ^1H signals remain. The 7.8 ppm NH_3 signal also remains, as expected, due to the fast three-site jump motion of the amino group (Figure 2e). Finally, when both ^{13}C and ^{15}N dephasing pulses are turned on, all resonances except for the 7.8 ppm H N signal are suppressed (Figure 2f). These spectra thus confirm the ability of the MELODI–HETCOR experiment to remove the ^1H signals of rigid segments, leaving only the signals of mobile protons and nonprotein protons in the spectra.

Water Interaction with an Arg Side Chain of Membrane-Bound PG-1. To investigate whether the Arg $_4$ side chain in PG-1 is solvated by water in the lipid membrane, we first verify that Arg $_4$ is well-inserted into the hydrocarbon region of the lipid membrane. Previous paramagnetic relaxation enhancement⁴⁵ and ^1H spin diffusion experiments⁴⁶ showed that PG-1 adopts a TM orientation in neutral DLPC and POPC bilayers, with increasing depths of immersion for $\text{G2} < \text{F12} < \text{L5} \approx \text{V16}$. In anionic lipid membranes, ^{13}C – ^{31}P distances²⁵ and ^1H spin diffusion data³² showed that Leu $_5$ is in close contact with both the lipid chains and the headgroups, indicating that the lipid membrane forms a toroidal pore near the peptide. Since Arg $_4$ is adjacent to Leu $_5$, it should also be in close contact with the acyl chains. Figure 4 shows a 2D ^{13}C – ^1H HETCOR spectrum

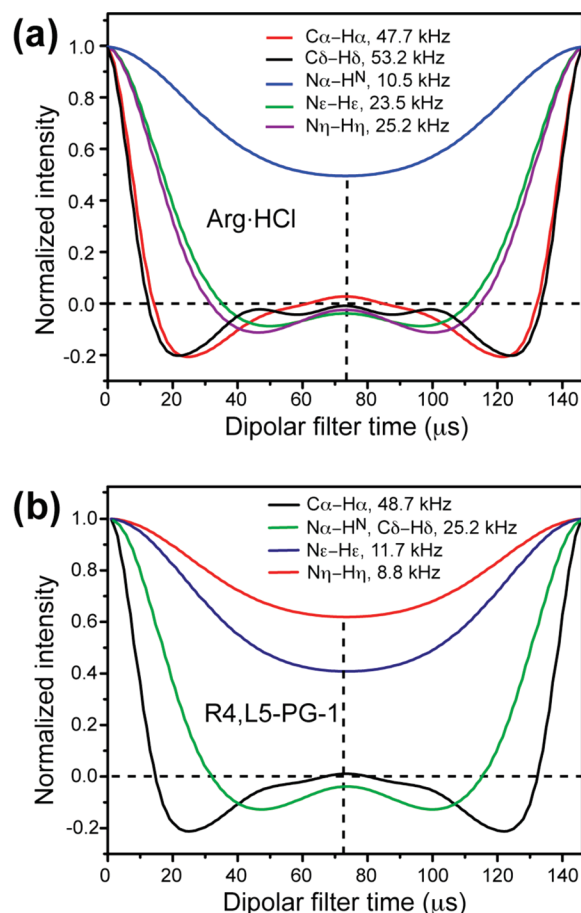


Figure 3. Simulated two-rotor-period MELODI–HETCOR dipolar dephasing curves of ^1H spins bonded to ^{13}C or ^{15}N . An ideal FSLG scaling factor of 0.577³³ was assumed. The simulated coupling strengths were obtained as $\delta_{\text{XH}}^{\text{rigid}} \times 4 \times 0.577 \times S_{\text{XH}}$, where the rigid-limit couplings are $\delta_{\text{NH}}^{\text{rigid}} = 10.6$ kHz and $\delta_{\text{CH}}^{\text{rigid}} = 22.7$ kHz, and the order parameters were obtained from direct measurements. (a) Simulated curves for Arg \cdot HCl. C–H and N–H order parameters of 0.4 – 1.0 were used. (b) Simulated curves for R4, L5–PG-1 in POPE/POPG membranes. Order parameters varied from 0.36 to 1.0.

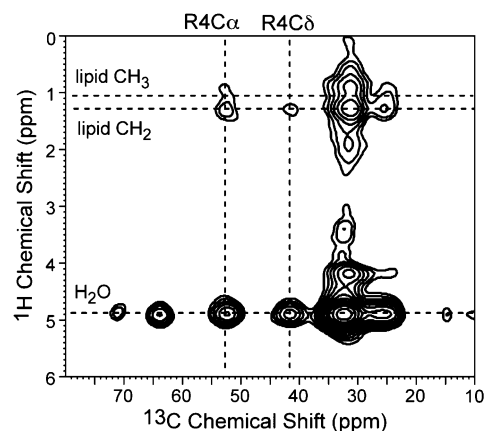


Figure 4. 2D ^{13}C -detected ^1H spin diffusion spectrum of R4, L5–PG-1 in POPE/POPG membrane at 283 K. A ^1H mixing time of 100 ms was used.

with 100 ms ^1H spin diffusion. The ^1H dimension was measured without homonuclear decoupling; thus, only signals of mobile water and lipids were detected. Weak but clear cross-peaks between Arg $_4$ C α /C δ and lipid CH_2 protons can be detected, indicating qualitatively that Arg $_4$ is inserted into the hydrocarbon region of the membrane. The spectrum also shows strong

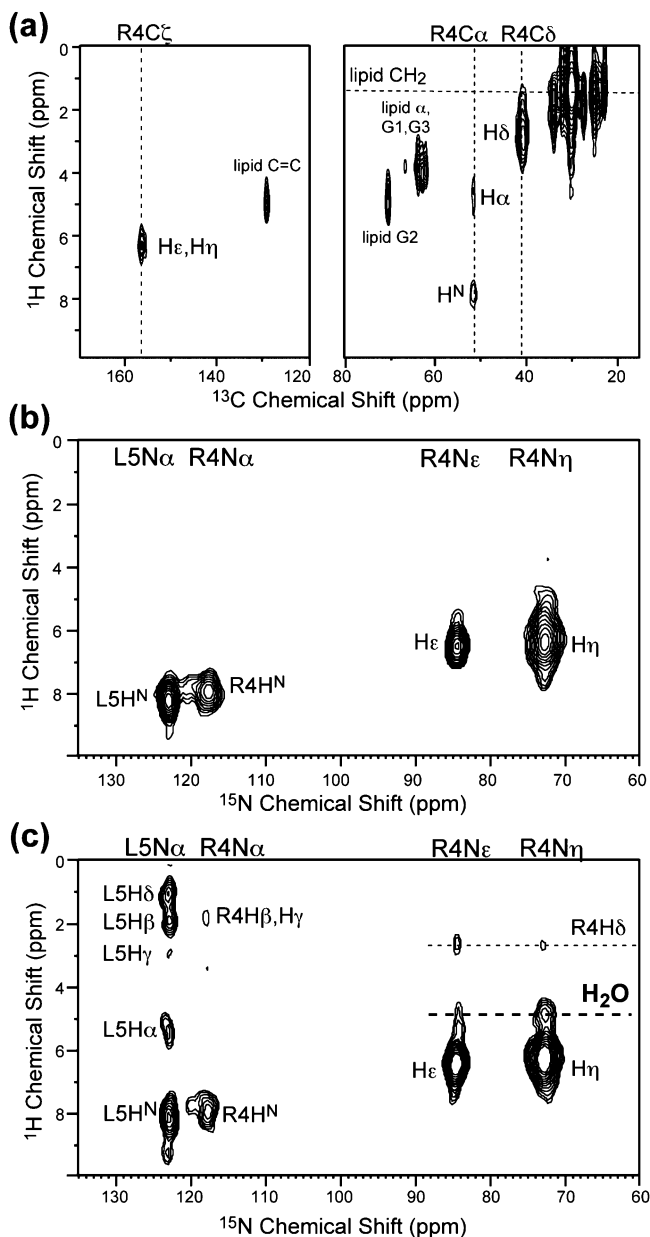


Figure 5. 2D HETCOR spectra of R4, L5-PG-1 in POPE/POPG membrane at 283 K. (a) ^1H – ^{13}C LG-HETCOR. (b) ^1H – ^{15}N LG-HETCOR. (c) ^1H – ^{15}N HH-HETCOR with 2 ms HH-CP and no ^1H mixing period.

Arg₄–water cross-peaks. However, at the long ^1H spin diffusion mixing time used, these water peaks may originate from water on the membrane surface rather than hydration water around the guanidinium. Thus, we carried out ^1H homonuclear-decoupled HETCOR experiments with short spin diffusion mixing time to detect water neighboring Arg₄.

Figure 5a,b displays the 2D ^1H – ^{13}C and ^1H – ^{15}N LG-HETCOR spectra of membrane-bound R4, L5-PG-1 at 283 K. Both peptide and lipid peaks can be readily assigned. The well-resolved lipid ^1H signals in the ^1H – ^{13}C 2D spectrum provided convenient chemical shift references for the peptide ^1H signals.⁴⁷ Arg₄ C α shows cross-peaks to directly bonded H α as well as amide H^N, which allows ^1H chemical shift calibration of the 2D ^1H – ^{15}N spectra. When ^1H spin diffusion was activated by the use of 2 ms HH-CP, the 2D ^1H – ^{15}N HH-HETCOR spectrum (Figure 5c) shows multiple-bond cross-peaks between the Leu₅ N α and its aliphatic protons. Arg₄ N ϵ and N η exhibit

not only directly bonded H ϵ and H η peaks, but also weak multibond cross-peaks with H δ (2.9 ppm).

In addition, a cross-peak at 4.8 ppm was detected. In principle, this 4.8 ppm peak may be due to (1) Arg₄ H α (4.5 ppm in the ^1H – ^{13}C HETCOR spectrum), (2) a guanidinium proton whose signal is weak in the ^1H – ^{15}N LG-HETCOR spectrum but stronger in the HH-HETCOR spectrum, or (3) water. To distinguish the three possibilities, we implemented ^{15}N and ^{13}C MELODI filters (Figure 6). When ^{15}N dephasing pulses were turned on for two rotor periods, the amide H^N–N α peaks of Arg₄ and Leu₅ were both suppressed, as expected. The N ϵ –H ϵ and N η –H η peaks decreased in intensities but did not disappear completely, indicating side chain motion at 283 K (Figure 6b). This side chain motion is consistent with previously measured Arg₄ guanidinium S_{NH} of 0.35–0.50,⁴⁴ which translates to effective dipole couplings of 25.2, 11.7, and 8.8 kHz for N α –H^N, N ϵ –H ϵ , and N η –H η during two rotor periods of ^{15}N MELODI filter. Figure 3b shows the calculated intensities for the three couplings: with the dephasing pulses at the center of each rotor period, the H^N, H ϵ , and H η intensities are –6%, 43%, and 64% of the full intensities. Thus, the complete suppression of the H^N peak and the reduced intensities of the guanidinium peaks in Figure 6b are qualitatively consistent with the calculated intensities. Figure 6b also shows that the multibond aliphatic proton–amide ^{15}N cross-peaks of Arg₄ and Leu₅ survived the ^{15}N MELODI filter, as expected. Moreover, the 4.8 ppm ^1H peak remained in the spectrum.

To effect stronger dipolar dephasing, we measured a four-rotor-period MELODI–HETCOR spectrum (Figure 6c), which further decreased the one-bond N ϵ –H ϵ and N η –H η peak intensities while retaining the intensity of the 4.8 ppm peak. Figure 6e compares the N ϵ and N η cross sections of the three 2D spectra, which show that the relative intensity of the 4.8 ppm peak increased from being only 10% of the one-bond peaks in the control spectrum to 30–50% in the two-rotor-period MELODI spectrum and to 70–100% of the one-bond peaks in the four-rotor-period MELODI spectrum. This trend rules out H η or H ϵ as the cause of the 4.8 ppm peak.

Finally, to test whether the 4.8 ppm peak is due to Arg₄ H α , we applied simultaneous ^{13}C , ^{15}N dephasing. The resulting 2D spectrum (Figure 6d) shows the clear retention of the 4.8 ppm peak and the removal of all Arg₄ aliphatic ^1H signals. In particular, the Arg₄ two-bond N α –H α peak is suppressed, indicating that ^{13}C dephasing is successful for removing the H α magnetization. Since Leu₅ is not labeled with ^{13}C , the Leu₅ aliphatic protons retain weak cross-peaks with the Leu₅ amide ^{15}N . Taken together, these dipolar edited HETCOR spectra indicate that Arg₄ N η correlates with water protons within a short ^1H mixing time of only 1 ms (due to 2 ms HH-CP). The fact that the backbone N α 's do not exhibit this 4.8 ppm cross-peak confirms the site-specific nature of the water molecules interacting with the guanidinium moiety.

Discussion

The above data demonstrate the feasibility of detecting site-specific interactions between water molecules and membrane proteins without requiring protein perdeuteration. So far, all solid-state NMR studies of protein–water interactions by heteronuclear correlation experiments have used perdeuterated proteins to avoid overlap of protein ^1H signals, primarily H α and H^N, with the water signal.^{2,4} However, protein perdeuteration is costly and sometimes infeasible. The ^{13}C or ^{15}N dipolar-edited MELODI–HETCOR experiment obviates the need for perdeuteration by suppressing the signals of all protons that are directly

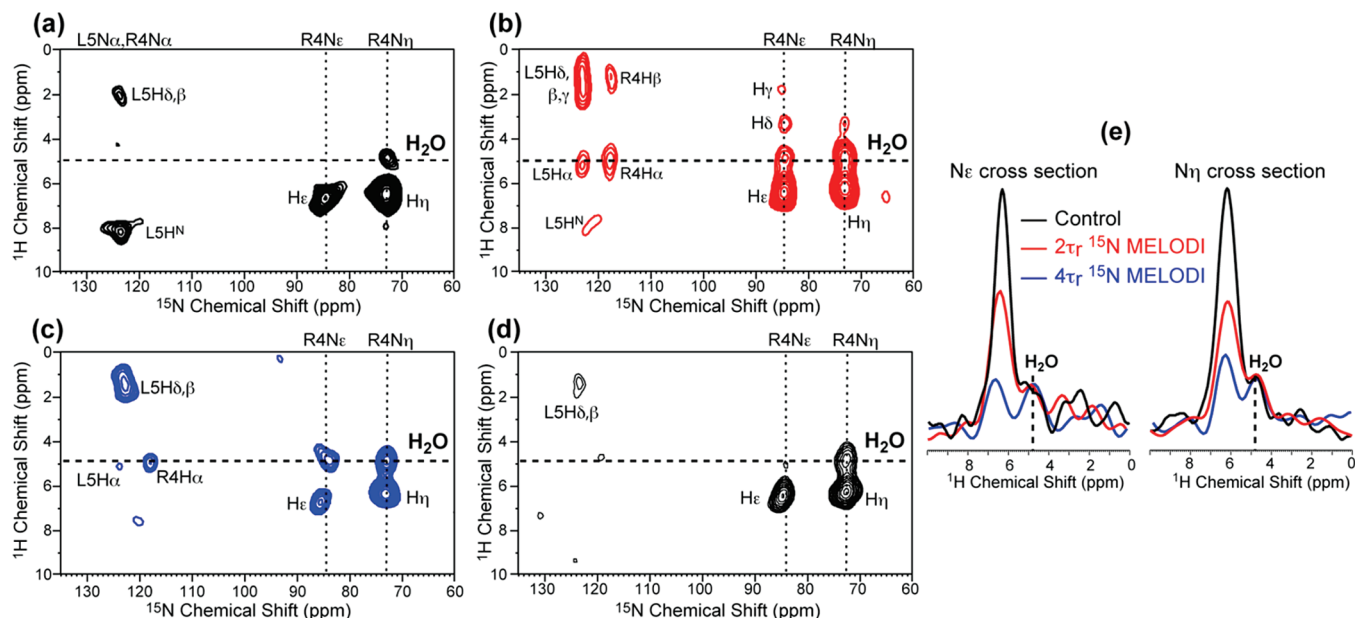


Figure 6. 2D ^1H – ^{15}N MELODI–HETCOR spectra of R4, L5–PG-1 in POPE/POPG membranes at 283 K. (a) HH-HETCOR spectrum. (b) MELODI–HETCOR spectrum with two rotor periods of ^{15}N dephasing. (c) MELODI–HETCOR spectrum with four rotor periods of ^{15}N dephasing. (d) MELODI–HETCOR spectrum with two rotor periods of simultaneous ^{13}C and ^{15}N dephasing. (e) ^1H cross sections of R4 N_ϵ and N_η extracted from spectra a–c.

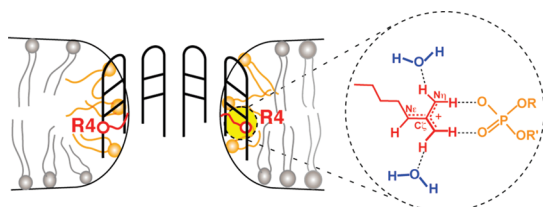


Figure 7. Illustration of Arg side chain interaction with lipids headgroups and water inside the membrane.

bonded to a ^{13}C or ^{15}N spin, leaving only intermolecular water or lipid ^1H resonances of interest. By restricting ^1H spin diffusion to a short period of 1 ms, one can largely suppress the intensity of remote membrane-surface water.^{7,9} The fact that the 4.8 ppm ^1H signal correlates with Arg₄ N_ϵ and N_η but not with the backbone N_α of Arg₄ and Leu₅ (Figure 6d) supports the site-specific nature of the observed water interaction with the guanidinium ion. The Arg₄-bound water is well-immersed into the hydrophobic region of the membrane, since both Arg₄ and Leu₅ are within spin diffusion contact with the lipid chains.

The observed Arg₄–water close contact inside the lipid membrane, combined with previous report of short Arg₄ guanidinium–phosphate distances,²⁵ indicates that PG-1 utilizes both lipid phosphates and water molecules to stabilize its Arg side chains in the hydrophobic core of the membrane (Figure 7). Each guanidinium group provides up to five hydrogen-bond donors, which can interact with the oxygen atoms of several phosphates and water molecules. Although the exact stoichiometry of water and phosphates per guanidinium is not known, our data indicate that both species must be present to solvate and neutralize the positively charged Arg₄ in the membrane. The toroidal pore morphology of the membrane near the peptide, caused by lipids that change their orientations to embed their phosphate groups near the arginine side chains, has been extensively characterized using static ^{31}P and ^2H NMR line-shapes and MD simulations for PG-1-bound membranes^{48–51} as well as for other membrane-active peptides.⁵²

The mechanism of water polarization transfer to Arg₄ in membrane-bound PG-1 is probably temperature-dependent. At

283 K, the most likely mechanism is chemical exchange, with previously reported exchange rates of $\sim 100\text{ s}^{-1}$ at pH 7 and 10–20 °C for Arg H_ϵ and H_η .⁵³ We also measured PG-1 HETCOR spectra at 253 K, where weak water cross-peaks were also detected (data not shown). At low temperature, chemical exchange becomes negligible ($\ll 10\text{ s}^{-1}$); thus, water polarization transfer to guanidinium most likely proceeds by dipolar spin diffusion. Previous solid-state NMR studies of microcrystalline proteins did not detect Arg–water correlations due to interresidue hydrogen bonding of the arginines with other residues.⁵⁴ PG-1 contains 33% Arg in its amino acid sequence (6 Arg residues out of 18 residues) and no acidic residues; thus, peptide–peptide interactions are clearly insufficient, if not completely absent, for stabilizing the Arg residues. Thus, it is not surprising that lipid headgroups and water molecules provide the necessary hydrogen-bond partners and solvation shells to these Arg's, as shown by the current 2D data and previous ^{13}C – ^{31}P distance results.

The observed guanidinium–water correlation provides direct experimental evidence for the proposal, based on MD simulations, that Arg residues in membrane proteins are solvated by water molecules pulled into the membrane. These simulations gave detailed insights about how Arg residues in model peptides and voltage-sensing helices of potassium channels may be stabilized in lipid bilayers. Most simulations agreed that Arg remains largely protonated across most of the lipid membrane. The aqueous pK_a of Arg is 12.5,⁵⁵ and a pK_a shift of 4.5 or less has been computed,²³ thus predicting that Arg remains predominantly protonated in the membrane at pH 7.²¹ Potentials of mean force calculations indicated that the protonated Arg is stabilized mainly by hydration water and to a smaller extent by lipid phosphates, both of which are pulled into the membrane.^{18,19} Large water defects that connect bulk water with the charged Arg side chain all the way to the center of the membrane were observed,²² and the core water molecules stabilize the Arg by as much as 35 kcal/mol.¹⁹ These water defects and embedded lipid headgroups cause significant membrane deformation.^{17,19} In the case of PG-1, such membrane deformation is manifested

by the ³¹P NMR spectra of PG-1-containing lipid membranes.^{49,56} The number of water molecules associated with each guanidinium in the membrane varies with the position of the Arg. For the S4 helix of a voltage-gated potassium channel, 1–3 water–guanidinium hydrogen bonds were detected in MD simulations up to 10 ns.¹⁷ For an Arg-containing poly-Leu helix, five water molecules were found to be coordinated to the Arg throughout the membrane.¹⁸ The Arg-coordinated water is suggested to be more sluggish than bulk water, with 200–300 times longer mean residence times in the case of the S4 helix.¹⁷

Conclusion

The current HETCOR solid-state NMR study provides the first experimental evidence for site-specific guanidinium–water interaction in an Arg-rich membrane peptide that is well-inserted into the lipid membrane. The ¹³C, ¹⁵N-dephased MELODI–HETCOR experiment unambiguously distinguishes intermolecular water–Arg cross-peaks from intramolecular peptide cross-peaks. Varying the dipolar dephasing time in the MELODI–HETCOR experiment also distinguishes the signals of mobile protein segments from intermolecular water–Arg cross-peaks. The membrane-inserted water is able to transfer its polarization to the Arg side chain within 1 ms; thus, it is in close proximity to the guanidinium and may form transient water–guanidinium hydrogen bonds. Together with previous results of short Arg–phosphate distances²⁵ indicative of the presence of highly curved toroidal pores in the membrane, these solid-state NMR data indicate that Arg side chains in the β-hairpin PG-1 utilize water for charge solvation and lipid phosphates for charge neutralization, thus stabilizing the insertion of the peptide across the lipid membrane. The resulting membrane deformation provides the structural basis for the membrane-disruptive function of PG-1.

Acknowledgment. This work is supported by an NIH grant, GM66976, to M.H. and an NSF instrumentation grant, DBI421374, for the 600 MHz NMR at Iowa State University.

References and Notes

- Otting, G. *Prog. Nucl. Magn. Reson. Spectrosc.* **1997**, *31*, 259.
- Lesage, A.; Bockmann, A. *J. Am. Chem. Soc.* **2003**, *125*, 13336.
- Paulson, E. K.; Morcombe, C. R.; Gaponenko, V.; Dancheck, B.; Byrd, R. A.; Zilm, K. W. *J. Am. Chem. Soc.* **2003**, *125*, 14222.
- Lesage, A.; Emsley, L.; Penin, F.; Bockmann, A. *J. Am. Chem. Soc.* **2006**, *128*, 8246.
- Lesage, A.; Gardienet, C.; Loquet, A.; Verel, R.; Pintacuda, G.; Emsley, L.; Meier, B. H.; Bockmann, A. *Angew. Chem., Int. Ed.* **2008**, *47*, 5851.
- Kumashiro, K. K.; Schmidt-Rohr, K.; Murphy, O. J.; Ouellette, K. L.; Cramer, W. A.; Thompson, L. K. *J. Am. Chem. Soc.* **1998**, *120*, 5043.
- Huster, D.; Yao, X. L.; Hong, M. *J. Am. Chem. Soc.* **2002**, *124*, 874.
- Luo, W. B.; Hong, M. *Solid State Nucl. Magn. Reson.* **2006**, *29*, 163.
- Ader, C.; Schneider, R.; Seidel, K.; Etzkorn, M.; Becker, S.; Baldus, M. *J. Am. Chem. Soc.* **2009**, *131*, 170.
- Jiang, Y. X.; Ruta, V.; Chen, J. Y.; Lee, A.; MacKinnon, R. *Nature* **2003**, *423*, 42.
- Long, S. B.; Tao, X.; Campbell, E. B.; MacKinnon, R. *Nature* **2007**, *450*, 376.
- Swartz, K. J. *Nature* **2008**, *456*, 891.
- Tang, M.; Waring, A. J.; Lehrer, R. I.; Hong, M. *Angew. Chem., Int. Ed.* **2008**, *47*, 3202.
- Epand, R. M.; Vogel, H. J. *Biochim. Biophys. Acta* **1999**, *1462*, 11.
- Fischer, R.; Fotin-Mleczek, M.; Hufnagel, H.; Brock, R. *Chem-BioChem* **2005**, *6*, 2126.
- Hessa, T.; Kim, H.; Bihlmaier, K.; Lundin, C.; Boekel, J.; Andersson, H.; Nilsson, I.; White, S. H.; von Heijne, G. *Nature* **2005**, *433*, 377.
- Freites, J. A.; Tobias, D. J.; von Heijne, G.; White, S. H. *Proc. Natl. Acad. Sci. U.S.A.* **2005**, *102*, 15059.
- Li, L. B.; Vorobyov, I.; Allen, T. W. *J. Phys. Chem. B* **2008**, *112*, 9574.
- Dorairaj, S.; Allen, T. W. *Proc. Natl. Acad. Sci. U.S.A.* **2007**, *104*, 4943.
- Herce, H. D.; Garcia, A. E. *Proc. Natl. Acad. Sci. U.S.A.* **2007**, *104*, 20805.
- Yoo, J.; Cui, Q. *Biophys. J.* **2008**, *94*, L61.
- MacCallum, J. L.; Bennett, W. F. D.; Tieleman, D. P. *Biophys. J.* **2008**, *94*, 3393.
- Li, L.; Vorobyov, I.; MacKerell, A. D.; Allen, T. W. *Biophys. J.* **2008**, *94*, L11.
- Su, Y.; Doherty, T.; Waring, A. J.; Ruchala, P.; Hong, M. *Biochemistry* **2009**, *48*, 4587.
- Tang, M.; Waring, A. J.; Hong, M. *J. Am. Chem. Soc.* **2007**, *129*, 11438.
- Bellm, L.; Lehrer, R. I.; Ganz, T. *Expert Opin. Invest. Drugs* **2000**, *9*, 1731.
- Kokryakov, V. N.; Harwig, S. S. L.; Panyutich, E. A.; Shevchenko, A. A.; Aleshina, G. M.; Shamova, O. V.; Korneva, H. A.; Lehrer, R. I. *FEBS Lett.* **1993**, *327*, 231.
- Lehrer, R. I.; Barton, A.; Ganz, T. *J. Immunol. Methods* **1988**, *108*, 153.
- Sokolov, Y.; Mirzabekov, T.; Martin, D. W.; Lehrer, R. I.; Kagan, B. L. *Biochim. Biophys. Acta* **1999**, *1420*, 23.
- Ternovsky, V. I.; Okada, Y.; Sabirov, R. Z. *FEBS Lett.* **2004**, *576*, 433.
- Yang, L.; Weiss, T. M.; Lehrer, R. I.; Huang, H. W. *Biophys. J.* **2000**, *79*, 2002.
- Mani, R.; Cady, S. D.; Tang, M.; Waring, A. J.; Lehrer, R. I.; Hong, M. *Proc. Natl. Acad. Sci. U.S.A.* **2006**, *103*, 16242.
- Bielecki, A.; Kolbert, A. C.; de Groot, H. J. M.; Griffin, R. G.; Levitt, M. H. *Adv. Magn. Reson.* **1990**, *14*, 111.
- Rienstra, C. M.; Hohwy, M.; Hong, M.; Griffin, R. G. *J. Am. Chem. Soc.* **2000**, *122*, 10979.
- Rienstra, C. M.; Tucker-Kellogg, L.; Jaroniec, C. P.; Hohwy, M.; Reif, B.; McMahon, M. T.; Tidor, B.; Lozano-Perez, T.; Griffin, R. G. *Proc. Natl. Acad. Sci. U.S.A.* **2002**, *99*, 10260.
- Angell, C. A.; Shuppert, J.; Tucker, J. C. *J. Phys. Chem.* **1973**, *77*, 3092.
- Matubayasi, N.; Wakai, C.; Nakahara, M. *Phys. Rev. Lett.* **1997**, *78*, 2573.
- Lee, M.; Goldburg, W. I. *Phys. Rev.* **1965**, *140*, A1261.
- Yao, X. L.; Schmidt-Rohr, K.; Hong, M. *J. Magn. Reson.* **2001**, *149*, 139.
- Yao, X. L.; Hong, M. *J. Biomol. NMR* **2001**, *20*, 263.
- Gullion, T.; Schaefer, J. J. *Magn. Reson.* **1989**, *81*, 196.
- Mazumdar, S. K.; Venkates, K.; Mez, H. C.; Donohue, J. Z. *Kristallogr., Kristallphys., Kristallchem.* **1969**, *130*, 328.
- Petkova, A. T.; Hu, J. G. G.; Bizounok, M.; Simpson, M.; Griffin, R. G.; Herzfeld, J. *Biochemistry* **1999**, *38*, 1562.
- Tang, M.; Waring, A. J.; Hong, M. *ChemBioChem* **2008**, *9*, 1487.
- Buffy, J. J.; Hong, T.; Yamaguchi, S.; Waring, A. J.; Lehrer, R. I.; Hong, M. *Biophys. J.* **2003**, *85*, 2363.
- Buffy, J. J.; Waring, A. J.; Lehrer, R. I.; Hong, M. *Biochemistry* **2003**, *42*, 13725.
- Doherty, T.; Hong, M. *J. Magn. Reson.* **2009**, *196*, 39.
- Mani, R.; Buffy, J. J.; Waring, A. J.; Lehrer, R. I.; Hong, M. *Biochemistry* **2004**, *43*, 13839.
- Mani, R.; Waring, A. J.; Lehrer, R. I.; Hong, M. *Biochim. Biophys. Acta* **2005**, *1716*, 11.
- Wi, S.; Kim, C. *J. Phys. Chem. B* **2008**, *112*, 11402.
- Jang, H.; Ma, B.; Lal, R.; Nussinov, R. *Biophys. J.* **2008**, *95*, 4631.
- Agrawal, P.; Kiihne, S.; Hollander, J.; Hofmann, M.; Langosch, D.; de Groot, H. *Biochim. Biophys. Acta* **2010**, *1798*, 202.
- Liepinsh, E.; Otting, G. *Magn. Reson. Med.* **1996**, *35*, 30.
- Bockmann, A.; Juy, M.; Bettler, E.; Emsley, L.; Galinier, A.; Penin, F.; Lesage, A. *J. Biomol. NMR* **2005**, *32*, 195.
- Cantor, C. R.; Shimmel, P. R. *Biophysical Chemistry: Techniques for the Study of Biological Structure and Function*; Freeman: San Francisco, 1980.
- Yamaguchi, S.; Hong, T.; Waring, A.; Lehrer, R. I.; Hong, M. *Biochemistry* **2002**, *41*, 9852.